GCA-TR-69-7-N

ABSORPTION CROSS SECTIONS OF MINOR CONSTITUENTS IN PLANETARY ATMOSPHERES FROM 1050 TO 2100Å

By J. A. R. Samson
J. A. Myer

GCA CORPORATION
GCA TECHNOLOGY DIVISION
Bedford, Massachusetts

Dr. F. F. Marmo, Project Director and
Principal Investigator

November 1969

TABLE OF CONTENTS

ABSORPTION CROSS SECTIONS OF MINOR CONSTITUENTS
IN PLANETARY ATMOSPHERES FROM 1050 TO 2100Å

By J. A. R. Samson and J. A. Myer
GCA Corporation, GCA Technology Division
Bedford, Massachusetts

SUMMARY

The absorption cross sections of the following gases have been measured in the wavelength range 1050 to 2200Å: O_2, NO, I_2, HCℓ, CO, CO_2, SO_2, H_2O, ICN, NH_3, CH_4. Curves are presented of the cross sections as a function of wavelength for each gas with a short description of the important absorption features.
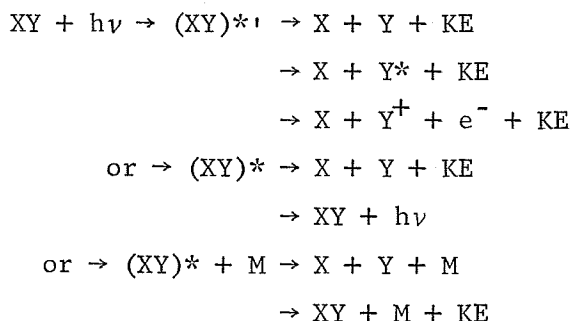
INTRODUCTION

The atmospheric absorption of solar ultraviolet radiation by constituent gases is of prime importance in the study of planetary atmospheres. These constituents, even in many of the cases when they are relatively minor ones, will play a significant role in the optical characteristics of the atmospheres.

We have measured the absorption cross sections in the region 1050 to 2200Å of a number of gases that are possible atmospheric constituents. The absorption spectra of many of these possible constituents, especially the minor ones, have not been measured under high resolution and it is possible that they may be significant absorbers in some regions of the spectrum. This could be particularly true in the spectral regions where the absorption properties of the major constituents are relatively weak and the minor constituents have very strong absorption features. In some cases, these possible strong features would be due to resonance bands belonging to Rydberg series. They would be anticipated to be very sharp discrete bands thus emphasizing the need for high resolution in their measurement.

Since most of the available data between 1050 and 2200Å for many of the more prominent atmospheric gases have been obtained with somewhat poorer resolution than we currently have available ($\sim$0.2Å), it was decided to remeasure the absorption cross sections of several of the better known major constituents. We would also be able to report this information in a standardized linear fashion for all gases, which is not the case for much of the previous cross section work scattered throughout the literature.

This improvement in spectral resolution is very important in determining the more accurate cross sections for sharp absorption features as well as in aiding any interpretation of the physical mechanisms responsible for the observed features. As an example of this, we were able to demonstrate in several cases that there were no significant continua underlying tightly spaced groups of bands as had been reported previously.

The interpretation of vacuum uv absorption spectra is a field where there is a definite need for improvement, since we are unable to predict for many molecules, whether an absorption feature is caused by molecular dissociation, predissociation, ionization, or resonance excitation as illustrated by the following mechanisms.

$$XY + h\nu \rightarrow (XY)^{*\prime} \rightarrow X + Y + KE$$
$$\rightarrow X + Y^* + KE$$
$$\rightarrow X + Y^+ + e^- + KE$$
$$or \rightarrow (XY)^* \rightarrow X + Y + KE$$
$$\rightarrow XY + h\nu$$
$$or \rightarrow (XY)^* + M \rightarrow X + Y + M$$
$$\rightarrow XY + M + KE$$

In the above scheme, $^{*\prime}$ denotes excitation to a transitory (repulsive) state which decomposes in its first vibration and * denotes normal excitation to a discrete electronic level which may or may not predissociate or autoionize. There are many more possible reaction paths but the above are a few of the more important ones.

Knowledge of the physical mechanism responsible for an absorption feature is extremely important in improving our understanding of the effective processes and reactions of planetary atmospheres. Information defining the product radical of a given photodissociation, the energy distribution of the products, the possibility of their reacting with other species to form new products, etc., is extremely important in interpreting atmospheric parameters. Because of this, an attempt has been made where possible, in the description and analysis of our spectra, to interpret them in terms of the possible or probable mechanisms. No attempt has been made to provide a comprehensive analysis of the data or to compare the cross sections with any of the previously published material.

We have also attempted to present the data graphically in as simple and standardized format as possible. The cross sections were all measured linearly in units of megabarns ($1Mb \equiv 10^{-18}$ cm^2) and were measured over the range 1050 to 2200Å, above which the absorption was found to be quite weak. It is hoped that with this standard method of graphical presentation one can have quick and simple access to absorption cross sections of many possible atmospheric constituents.

The measurement of absorption cross sections is based on the Lambert-Beer law,

$$I_\lambda = I_{0\lambda} \exp(-\sigma_\lambda n L),$$

where $I_{0\lambda}$ is the incident flux of wavelength λ, I_λ is the flux transmitted through the absorbing gas, σ_λ is the absorption cross section, n is the molecular density of the absorbing gas, and L is the absorption path length.

The absorption cross section is related to the absorption coefficient k_λ by the relationship $\sigma_\lambda = k_\lambda/n_0$ where n_0 is Loschmidt's number $(2.7 \times 10^{19}$ molecules/cm^3 at STP).

The Lambert-Beer law is valid only for truly monochromatic radiation of infinitely narrow bandpass. However, if the absorption cross section does not vary or is a slowly varying function of the wavelength over a given bandpass $\Delta\lambda$, an effective cross section can be measured for this bandpass. This technique can be readily applied to smooth absorption continua.

The situation is much more complicated in the spectral regions where there is sharp discrete structure. Unless the instrumental bandwidth is less than the width of the spectral features, true cross sections cannot be obtained. Previously the criterion to obtain true cross sections was based on the observations of the pressure dependence of the cross sections. That is, Beer's law was assumed to be valid if a plot of $\ln(I/I_0)$ vs n was linear. The true cross section was then equal to the slope of the curve. If the instrumental bandwidth was greater than the line width of the discrete structure, the linearity relation did not hold and a "pressure effect" was observed. In this case, the common practice was to extrapolate these pressure dependent curves to zero pressure to obtain the true absorption cross sections. However, both these criteria can be misleading. Hudson and Carter (Ref. 1) have demonstrated that the absorption cross section can decrease rapidly by a fraction of 1 to 0.4 of its peak value as the ratio of the bandwidth to line width varies from 0 to 2, even though a straight line plot of $\ln(I/I_0)$ vs n can be obtained over this range.

The present experimental arrangement had a bandpass of 0.25Å which is at least two orders of magnitude wider than the Doppler width of any unperturbed rotational absorption line. It is thus important to remember that the maxima of the cross section data in the discrete or banded regions of the spectrum will represent lower limits, while the minima represent upper limits. In spite of these limitations, the data are still valid as a good guide to the relative intensities of different absorption regions.

INSTRUMENTATION

This work was accomplished with a McPherson Model 225 one meter, vacuum uv scanning monochromator. The instrument, in its present configuration, has a one meter radius of curvature and a 1200 L/mm grating, blazed at 1500Å. This gives a reciprocal dispersion of 8.3Å/mm.

The unique feature of the present experimental arrangement is a McPherson Model 665 double beam attachment that was incorporated with the monochromator. This attachment has two optical paths with identical absorption cells (one is a reference cell) and a vibrating mirror that alternately reflects the dispersed light beam through each cell. The alternating signals are measured by two independent photomultiplier tubes (EMI 9635 B with sodium salycilate coatings) and the logarithm of the ratio of the two signals is evaluated by a logarithmic ratiometer and then registered on a linear strip chart recorder. If a known gas pressure is introduced into one of the absorption cells whose length is accurately known, then the absorption cross section can be determined directly from the recording.

For this technique to be most effective, it is necessary for the optical paths including the window transmissions of the cells to be as identical as possible at all wavelengths considered. If the optical paths are properly balanced, then one will obtain a smooth horizontal base line for effective zero cross section when there is no absorbing gas in either cell. This perfect balancing was, in practice, difficult to attain as it is shown on the experimental traces. The major problem is to obtain perfectly matched LiF windows. However, by baking the windows it is possible to obtain a reasonably good base line that would introduce small inaccuracies of only a few percent at the lower end of the wavelength scale.

The light source was a McPherson 630 vacuum uv lamp. It is a DC capillary discharge source similar to the design by Hinteregger (Ref. 2). One electrode is water cooled while the other is cooled by forced air. The lamp was operated with hydrogen at a pressure of approximately 1 torr and at a current of about 400 mA. The hydrogen spectrum is a continuum down to about 1650Å. In the wavelength region 1050 to 1650Å, the spectrum is composed of a large number of very closely spaced lines. It was hoped that the high current and pressure would broaden the lines sufficiently so that they overlap thus creating an effective continuum. This is a critical requirement for cross sections since the absence of lines in the primary spectrum could result in serious anomalies in the absorption spectrum. The lamp was operated windowless with the gas flow through the monochromator entrance slit.

The gases and vapors to be studied were introduced and controlled with a gas filling system which included a needle leak value, a diffusion

pump and several vapor traps, a McLeod gauge, a thermocouple gauge (0-100 microns), and an oil monometer for pressures up to 30 torr. Vapors were introduced through a double stopcock-flask arrangement on the same system. The gas pressures for the cross section measurements were read with the oil monometer over the range from 0.05 torr - 30.00 torr ($\pm$ 0.05 torr) which was adequate for most of the measurements.

EXPERIMENTAL TECHNIQUE

With the instrumentation just described, the actual attainment of
the cross sectional data is relatively simple. After a good base line
has been obtained, a known pressure of gas is introduced into the ab-
sorption cell and the wavelength range of interest is scanned. Using
this trace as an indicator, gas can either be added to or taken away
from the cell to adjust the trace readings into the most accurate and
readable range. Because of the increased possible error at the extreme
ends of the cross section scale, it was decided to make the measurements
over one decade only. The traces were run for at least three different
absorption cell pressures and the cross sections for regions of continuous
absorption had to agree to well within experimental error before a trace
was felt to be reliable.

RESULTS

Carbon Monoxide

The band spectrum of CO has been reviewed in detail by Krupenie (Ref. 3). The review includes references up to and including 1965.

For wavelengths longer than 1200Å, the most dominant absorption feature is the CO fourth positive system that extends from about 1200 to 1544Å (see Figure 1). This system has been ascribed to an $A^1\Pi - X^1\Sigma$ transition and is degraded to the long wavelength side. In the absence of collisional quenching, absorption by this system results in the emission of fluorescence in the spectral region up to 2750Å. In the sharp peaks of these bands, extremely high resolution work (Ref. 4) has shown that there are many rotational lines which we are obviously unable to resolve. Because of the discrete nature of this structure, the absorption cross sections presented here represent lower limits. However, they are about a factor of four greater than those quoted by Watanabe, et al (Ref. 5) which reflects the higher resolution of the present work. The cross sections for several of the peaks were measured as a function of the gas pressure (varied by a factor of 2), and were found to be independent of the pressure. However, a considerable pressure effect was found for the less intense absorption region of the bands away from the head.

The improved resolution of our trace demonstrates that there is not a significant continuum underlying the 1300-1600Å region as was apparent in the data of Watanabe, et al (Ref. 5). The Cameron bands were detected in the region around 1900Å, but their absorption was so weak and unreliable that we did not include them in the data trace. The absorption cross sections of these bands have been reported by Thompson, et al (Ref. 6).

The region from 1150 to 1050Å had several strong and very sharp absorption bands belonging to the Rydberg states $(E^1\Pi, C^1\Sigma^+, B^1\Sigma^+)$ - $X^1\Sigma^+$. There also appears to be a case of dissociation continuum below 1100Å (the minimum wavelength necessary to dissociate CO is 1108Å. A weak continuum possibly does exist. However, the magnitude of the present apparent continuum is probably caused by a lack of resolution.

One other interesting feature of the fourth positive system is that the (14,0) band overlaps the Lyman α line (1215.67Å) (Ref. 4). The Lyman α radiation emitted by the sun has a line width of approximately 1Å (Ref. 7). Thus, any interaction of the solar Lyman α line with CO will certainly excite rotational members of the (14,0) band. Lyman α is an extremely strong solar emission line and resonance scattering by the (14,0) band could be of significance in the study of the scattering of solar radiation by atmospheres containing CO.
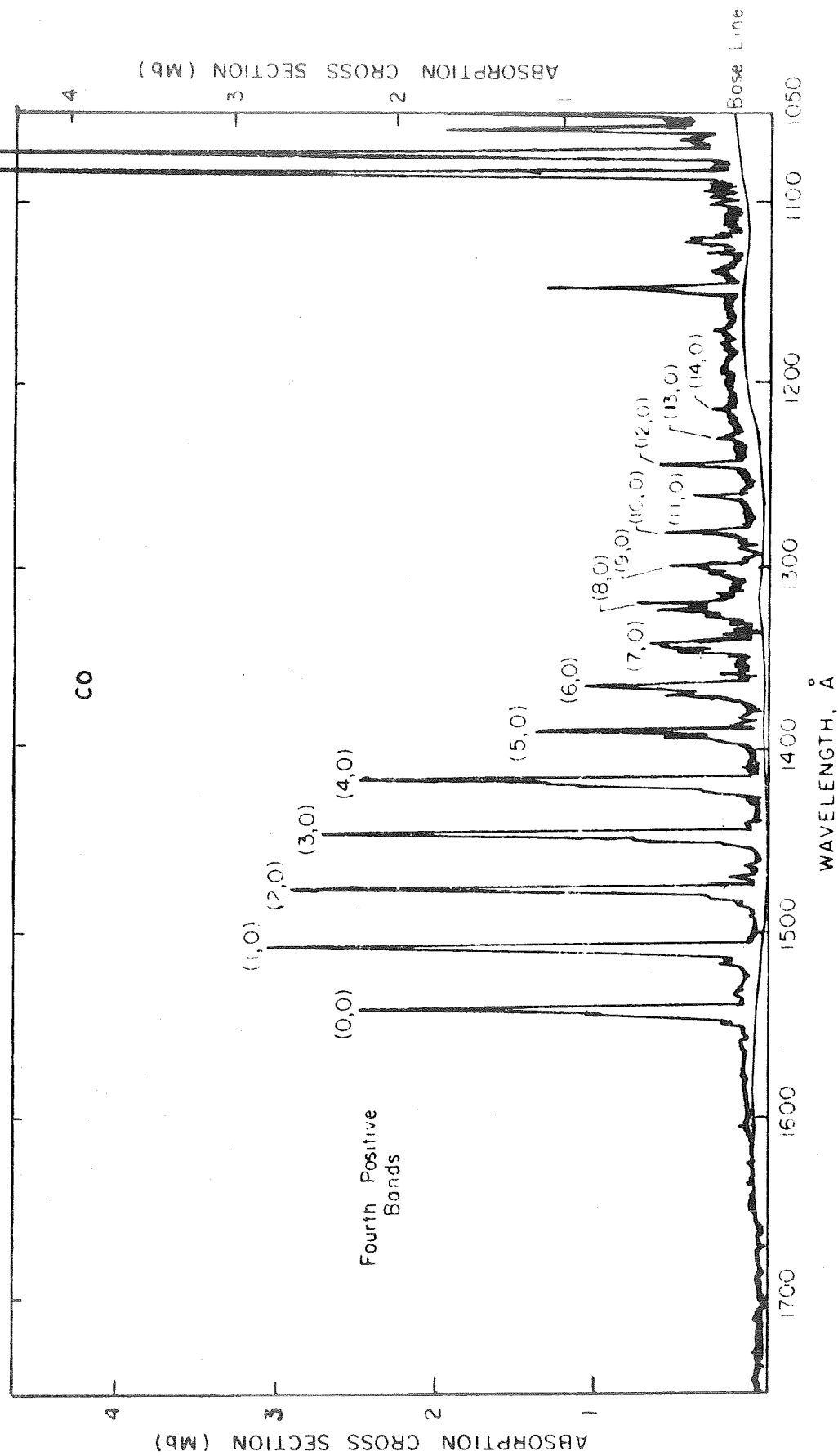
Figure 1. Absorption cross section of CO as a function of wavelength between 1750Å and 1050Å.

8

The vacuum uv spectrum of ammonia consists of four gross features or regions (see Figure 2). There has been considerable photochemical work done in this region. From 2200 to 1700Å, there is a broad feature that consists of a continuum overlapped by a series of broad, diffuse and un-resolvable bands. The photochemical reaction that has been reported for this feature is (Ref. 8):

$$NH_3 + h\nu \rightarrow NH_2 + H.$$
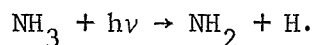
The extreme diffuseness of the apparent banded structure suggests that there is some predissociation mechanism operative.

The next region of interest is a series of very sharp bands be-tween 1650 and 1500Å. Neuimin and Terenin (Ref. 9) demonstrated that the following reactions occur in this region.

$$NH_3^* \rightarrow NH_2^* + H \ (\lambda < 1630Å),$$
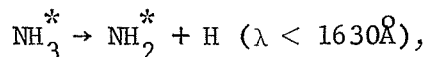
followed by
$$NH_2^* \rightarrow NH_2 + \alpha \text{ bands (fluorescence)}.$$

From the observations and apparent lack of continuum in this region, it seems probable that predissociation is the effective process.

Becker and Welge (Ref. 8) observed the fluorescence of the NH radical at 3250Å for $\lambda < 1470$Å in the following reaction.

$$NH_3 + h\nu \rightarrow NH^* \ (A^1\Pi, \ v' = 0) + H_2$$

$$NH^* \rightarrow NH + h\nu \ (A^1\Pi - X^1\Delta)$$
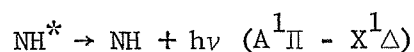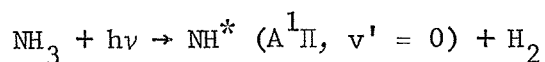
The spectral region from 1450 to 1200Å consists of strong, moder-ately broad bands overlapped on a relatively weak apparent continuum. This may only be an apparent continuum due to the lack of resolution or due to the smearing of the bands in predissociation.

At about 1230Å, there is the onset of a strong continuum with some weak structure superimposed on it. This continuum onset corresponds to the ionization threshold of ammonia and agrees with the photoionization data obtained by Watanabe (Ref. 10).

Methane

The structure of this spectrum appears to be continuous at all wave-lengths with very little sharp structure (see Figure 3). The first continuum onset is at about 1500Å and from there down the absorption is quite strong.
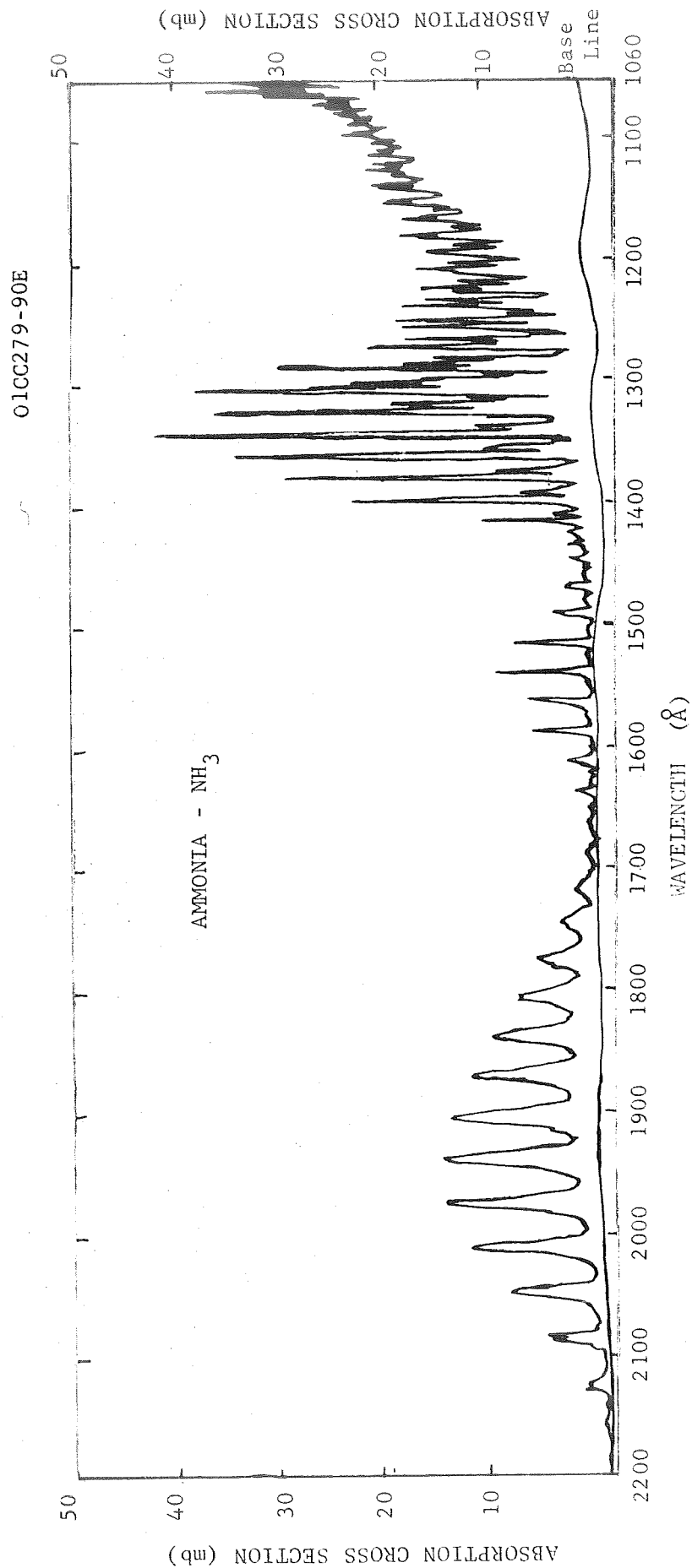
Figure 2. Absorption cross section of NH_3 as a function of wavelength between 2200Å and 1050Å.
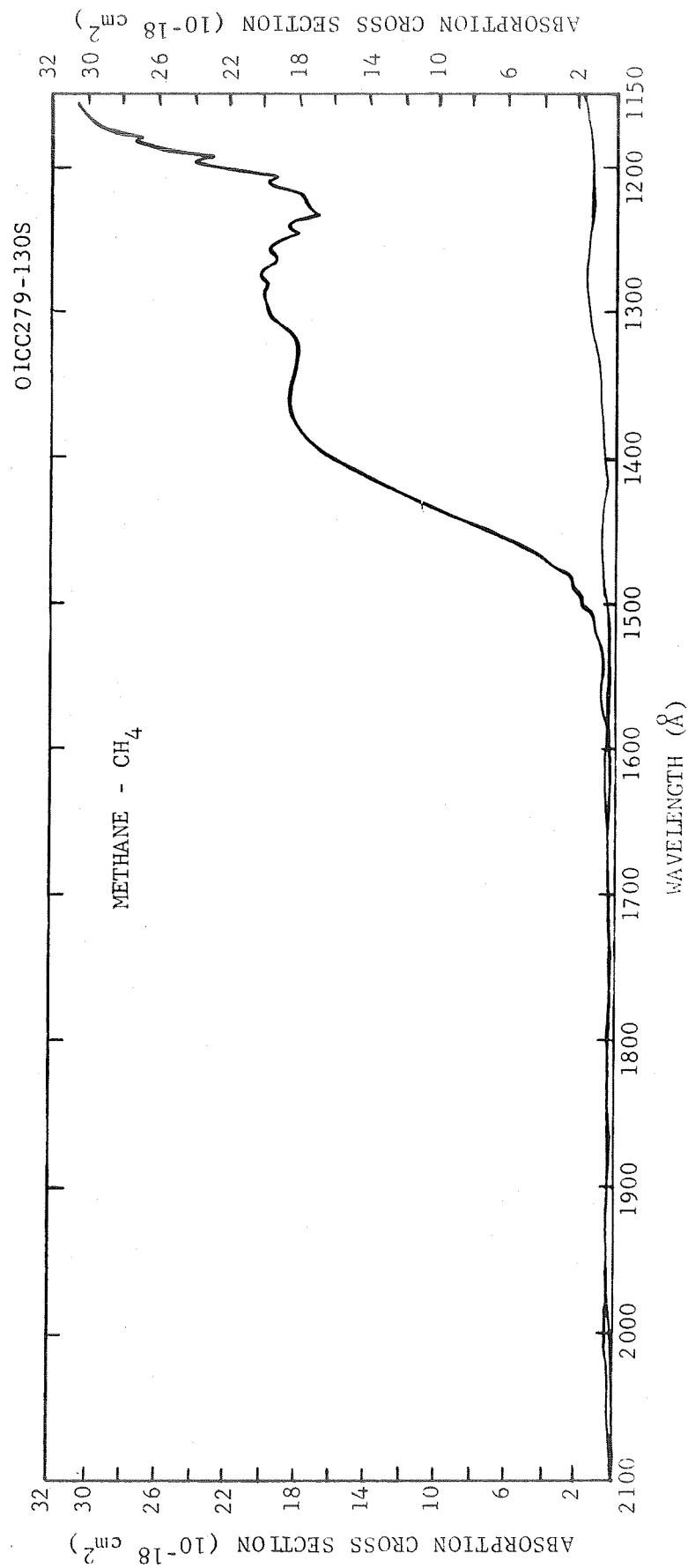
10

Figure 3. Absorption cross section of CH_4 as a function of wavelength between 2100Å to 1050Å.

At about 1230Å, there is an apparent onset of a much stronger continuous absorption with some weak structure superimposed on top of it.

Nitric Oxide

The region from 2200 to 1400Å contains a large number of overlapping vibrational bands belonging to the β, α, and δ resonance band systems. Several numbers of each of these systems are identified in Figure 4. The strongest bands belong to the δ system ($C^2\Pi - X^2\Pi$) which is a series of double headed bands degraded to shorter wavelength. The bands degraded to the red all belong to the β ($B^2\Pi - X^2\Pi$) system. The cross sections of these bands are probably only approximate as Marmo has reported a pressure effect (Ref. 11).

The region from 1350Å down consists of a relatively strong continuum superimposed with diffuse bands. The first ionization potential has been reported to be 1338Å (Ref. 12) which is in agreement with the onset of our observed continuum. This continuum has also been demonstrated to be partially due to photodissociation with N (^{2}D) and O (^{3}P) as the dissociation products. The cross section data of this region is in good agreement with Watanabe (Ref. 13).

Sulphur Dioxide

There is a broad absorption feature that extends from 1700 to 2200Å (see Figure 5). This entire region appears to have an underlying continuum with structure superimposed on it. The structure can be divided into two regions, one from 1930 to 2200Å and another from 1930 to 1700Å. The longer of these two regions is well defined band structure and has been described by Driscoll and Warneck (Ref. 14) as electronic excitation of SO_2. The second region consists of diffuse smeared bands and is probably a predissociation of some kind. The underlying continuum has been described as due to dissociation in the following reaction.

$$SO_2 + h\nu \rightarrow SO + O$$
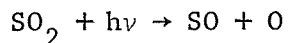
There is another continuum between 1330 and 1700Å region with diffuse and irregular structure superimposed on top of it. This continuum leads to a series of very strong bands from 1330Å that have been interpreted as resonance members in a Rydberg series converging to the ionization limit of 1006Å (Ref. 15). There is also a weak system in the 2000 to 3000Å region.

Water Vapor

There is a very broad structureless continuum that extends from 1440 to 1860Å that has been shown to be photodissociation yielding ground state hydroxyl radicals (see Figure 6), i.e.
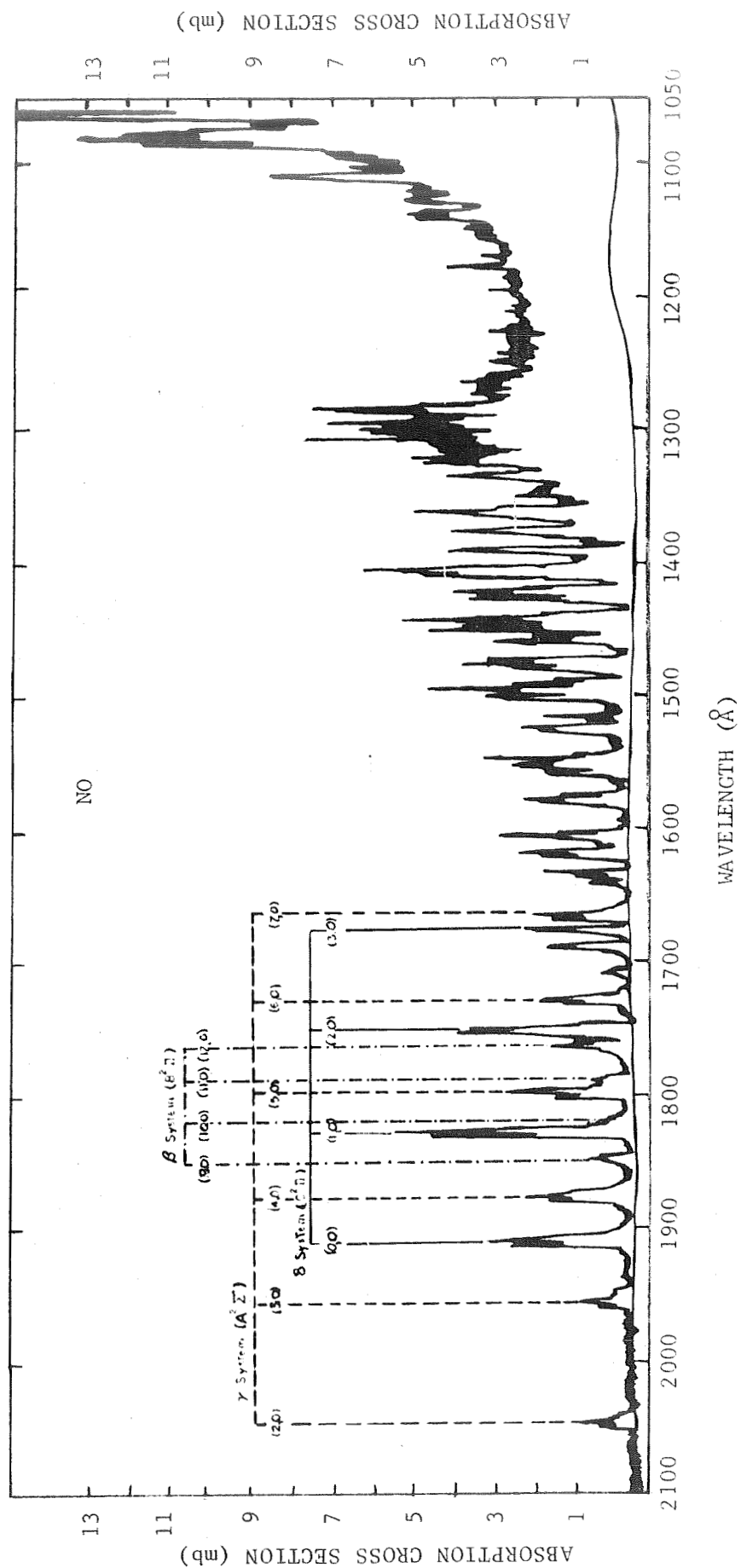
$$H_2O + h\nu \rightarrow H + OH \; (X^2\Pi)$$

12
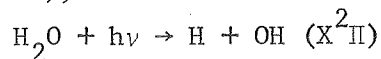
Figure 4. Absorption cross section of NO.
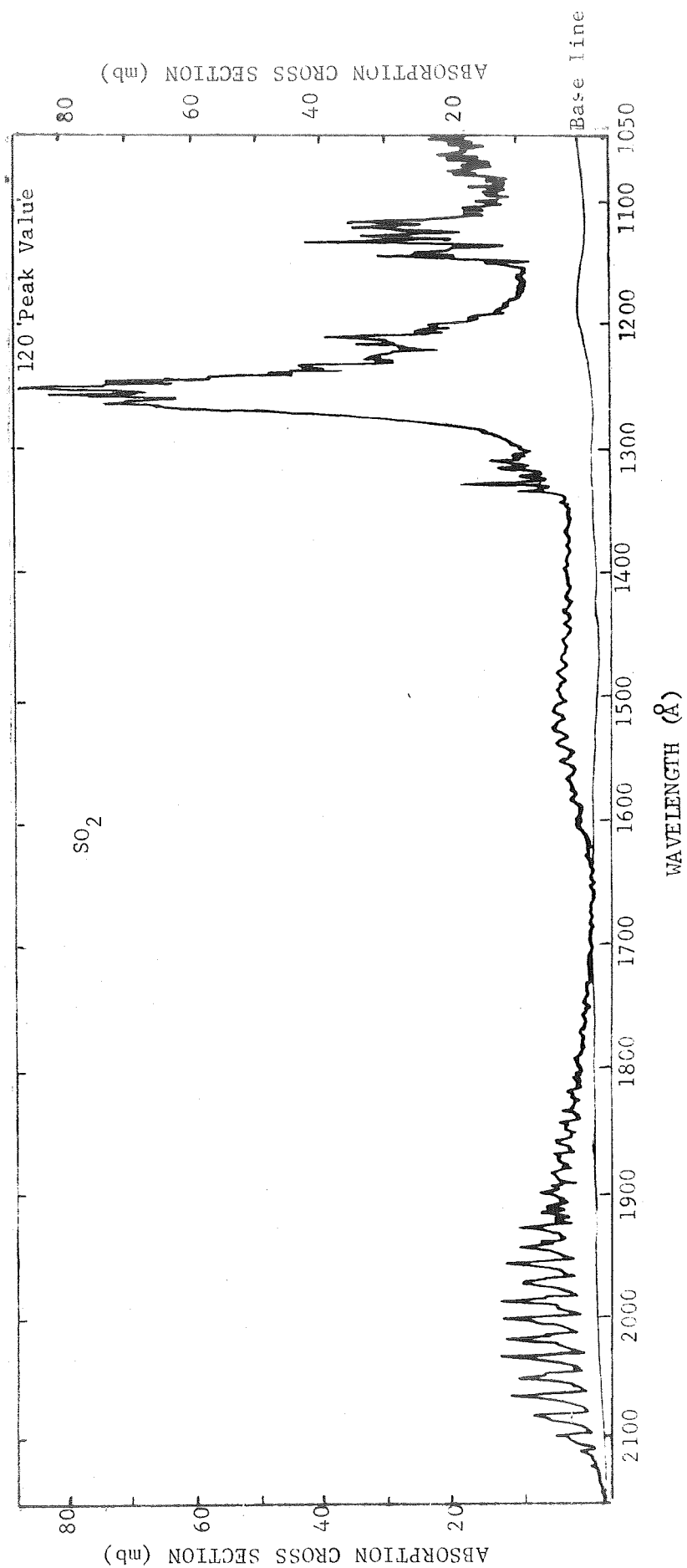
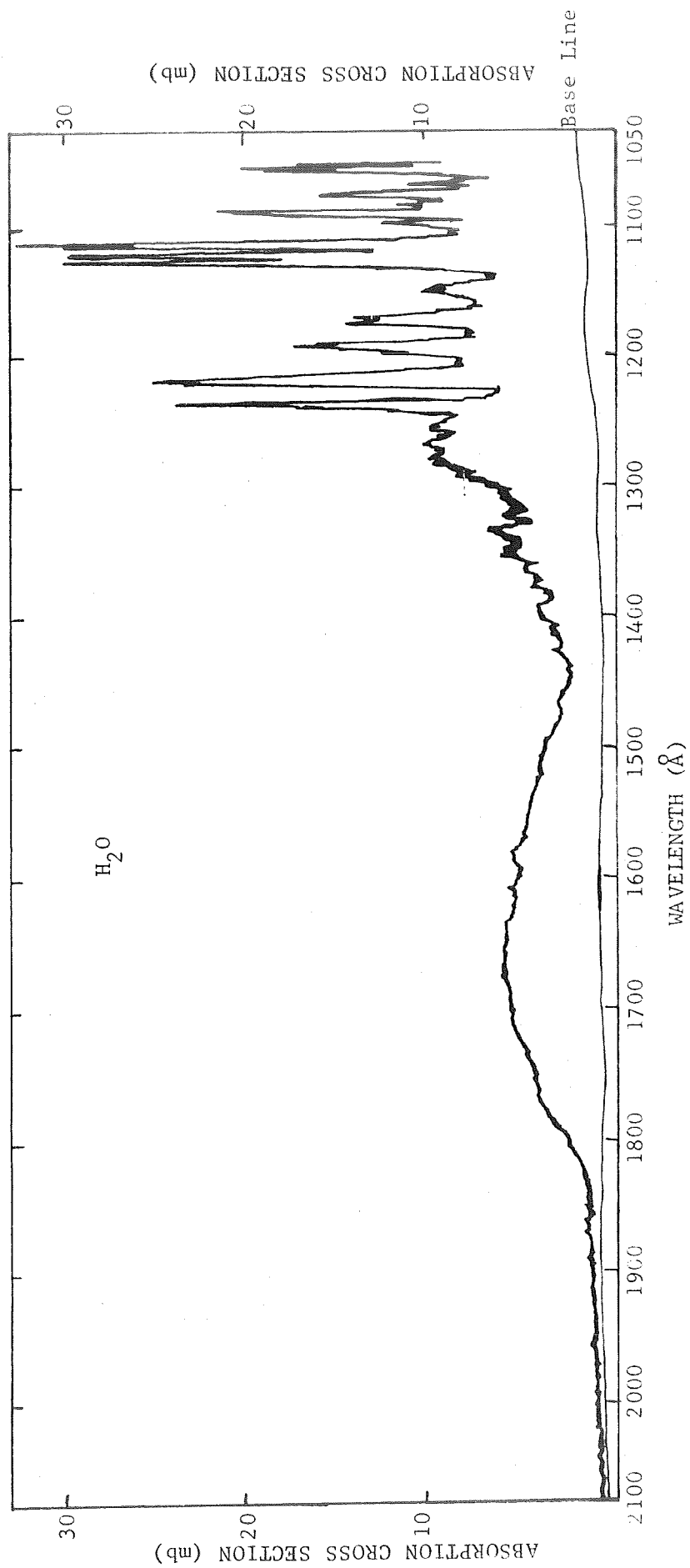Figure 5. Absorption cross section of SO_2.

Figure 6. Absorption cross section of H_2O.

15

At 1440Å, a second continuum begins and peaks at 1240Å where it merges into a series of irregular diffuse bands. At wavelengths less than 1350Å, it becomes energetically possible for the fragment radicals to be electronically excited and in fact fluorescence has been observed in the 3062Å (0,0) band of OH (Ref. 16).

$$H_2O + h\nu \rightarrow H + OH \ (A \ \Sigma^+)$$

and

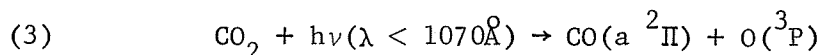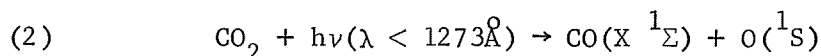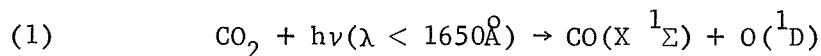$$OH \ (A \ ^2\Sigma^+) \rightarrow h\nu + OH \ (X \ ^2\Pi)$$
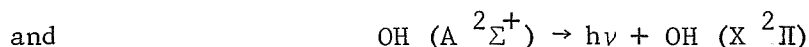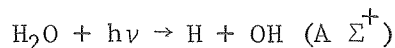
The first few bands from 1250 to 1150Å seem somewhat broadened and diffuse suggesting predissociation. The bands from 1150 to 1050Å are very sharp and strong and are resonance bands belonging to the Rydberg series which converges to 982Å.

Carbon Dioxide

There is a broad absorption feature of intermediate strength that extends from ~ 1350 to 1800Å that is probably caused by the overlapping of at least two continua that are superimposed with vibrational structure (see Figure 7). This vibrational structure above 1400Å is weak and very diffuse suggesting the possibility of predissociation. Below 1400Å, the structure is strong and much sharper.

At 1120Å and lower, there are several very strong and sharp features that appear to be continuous in some regions, but have been reported to be Rydberg terms (Ref. 17).

The reaction processes for this molecule are quite poorly understood. However, the following mechanisms are energetically possible.

(1) $$CO_2 + h\nu(\lambda < 1650Å) \rightarrow CO(X \ ^1\Sigma) + O(^1D)$$

(2) $$CO_2 + h\nu(\lambda < 1273Å) \rightarrow CO(X \ ^1\Sigma) + O(^1S)$$

(3) $$CO_2 + h\nu(\lambda < 1070Å) \rightarrow CO(a \ ^2\Pi) + O(^3P)$$

There is a definite need for further study of this molecule and its photochemical properties.

Oxygen

The dominant feature of the oxygen vacuum uv spectrum is the Schumann-Runge continuum and band system (see Figure 8 and 9). Absorption in the band system causes excitation to one of the vibrational levels of the $(^3\Sigma_u^-)$ state which crosses the energy curve of the $^3\Pi_u$ state and permits a predissociation mechanism to ground state oxygen atoms. That is

$$O_2(^3\Sigma_u^-) + h\nu \rightarrow O_2^*(^3\Sigma_u^-) \rightarrow O_2^*(^3\Pi_u) \rightarrow 2 \ O(^3P)$$
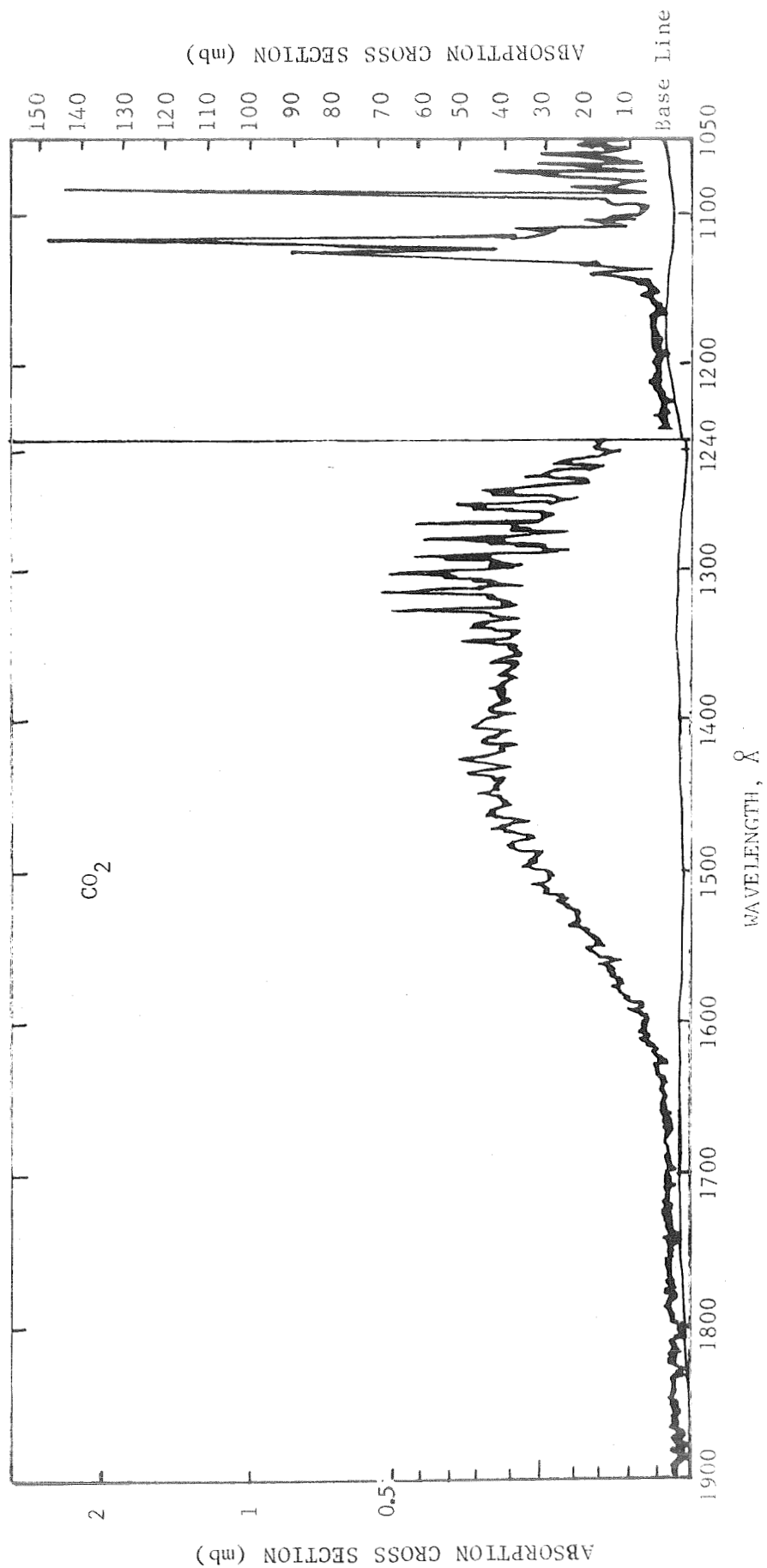
16
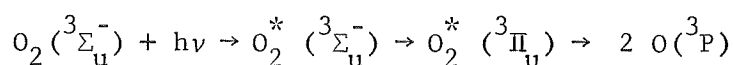
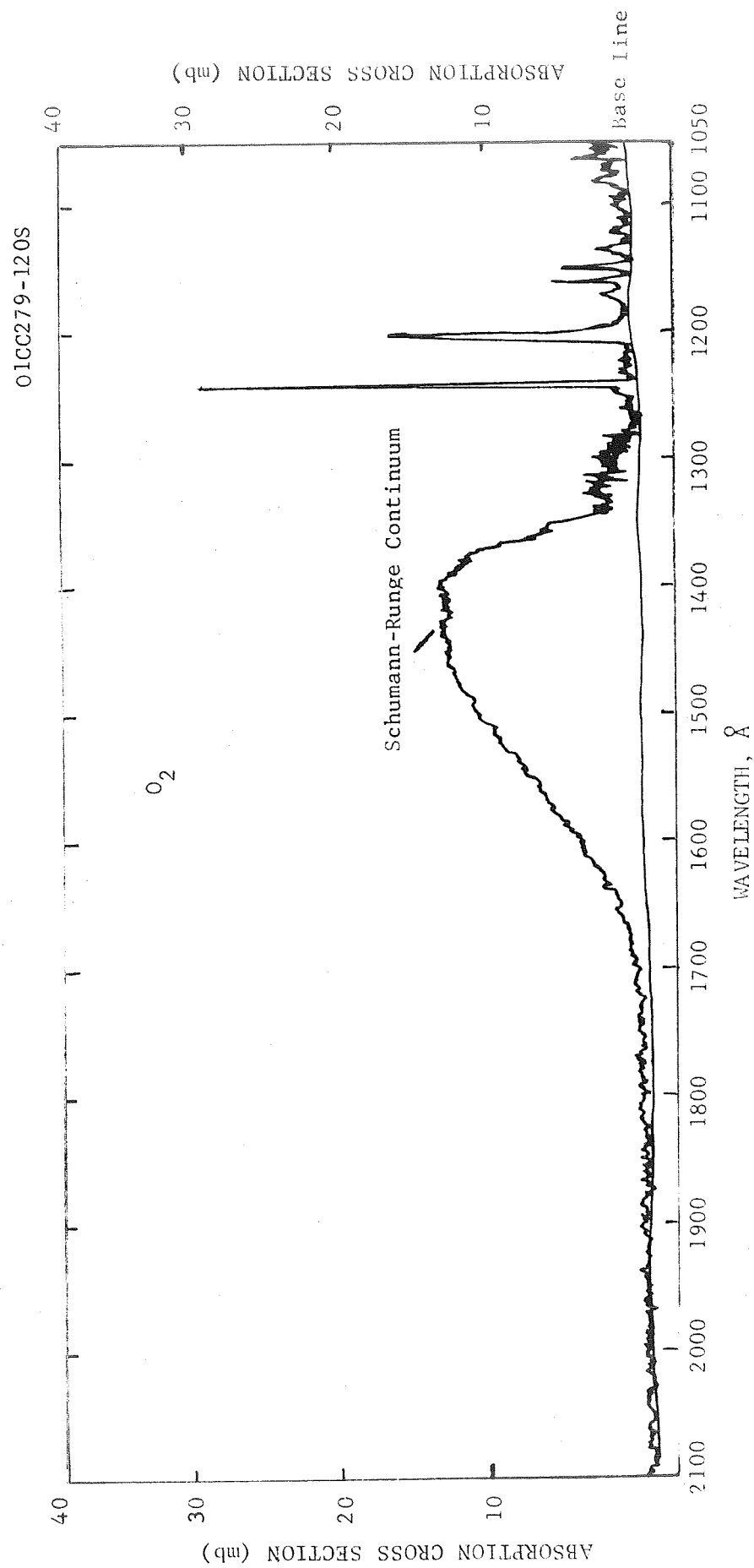Figure 7. Absorption cross section of CO_2 as a function of wavelength between 1900 and 1050Å.

Figure 8. Absorption cross section of O_2 as a function of wavelength between 2100 and 1050Å.
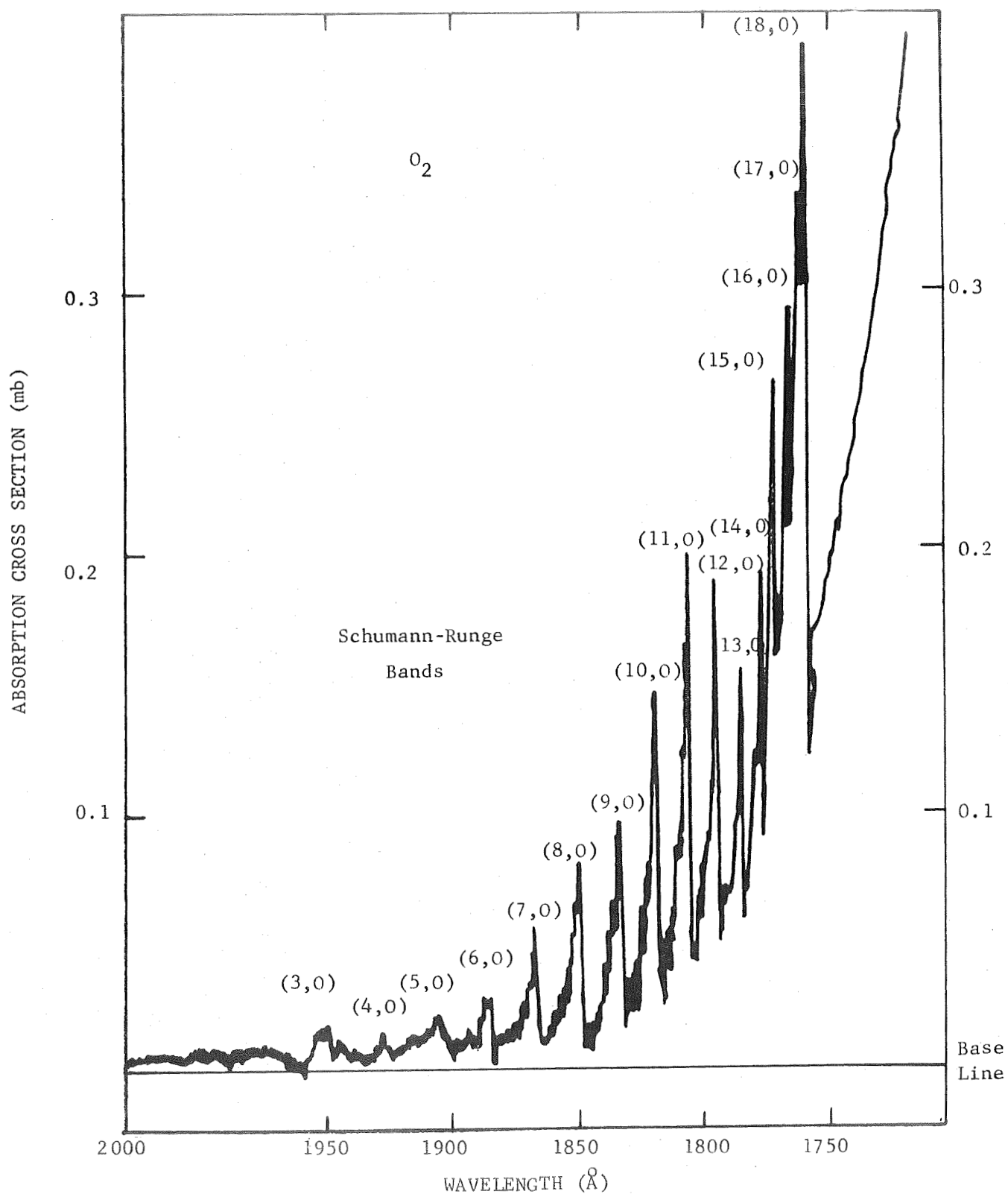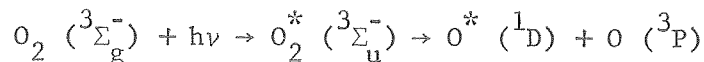
Figure 9.   Absorption cross section of O_2 as a function of wavelength
between 2000Å and 1750Å.

The following reaction is very likely responsible for the continuum.

$$O_2 \; (^3\Sigma_g^-) + h\nu \rightarrow O_2^* \; (^3\Sigma_u^-) \rightarrow O^* \; (^1D) + O \; (^3P)$$

The region from 1050 to about 1270Å is characterized by a series of irregular bands, some of considerable strength. Since the first ionization potential is at 1026Å, some of these bands are very likely members of the Rydberg series leading to this onset. The diffuseness of some of these bands suggests the possibility that they are also affected by predissociation.

Hydrogen Chloride

As a trace atmospheric constituent, HCℓ could be a very significant factor in the vacuum uv spectrum of planets. There is an extremely strong band system that was first detected by Price (Ref. 18) and denoted by him as the C state. This system has several vibrational members that have been identified as follows (see Figure 10):

$$
\begin{aligned}
(0,0) &\sim 1291.1\text{Å} \\
(1,0) &\sim 1247.3\text{Å} \\
(2,0) &\sim 1208.7\text{Å} \\
(3,0) &\sim 1175.0\text{Å}
\end{aligned}
$$

A vibrational analysis of these bands yields the following molecular constants,

$$\omega_e = 2880 \;\; \text{cm}^{-1}$$
$$\omega_e x_e = 80 \;\; \text{cm}^{-1},$$

which are in slight disagreement with those reported by Price. These bands are very sharp and well structured with very large absorption cross sections, especially for the (0,0) band which was measured (with some uncertainty due to pressure effect) to have a lower limit of 300 megabarns. We also observe the weak satellite bands that Price noted on the short wavelength side of each of these bands. In the absence of quenching collisions and predissociation, it is possible that these bands may also be observed strongly in fluorescence.

Price also identified a sharp band at 1330Å which he designated as the B state. This system does not appear to have any vibrational members or satellite bands. Both the B and C states are probably resonance Rydberg terms.

The region from 1150 to 1050Å has many overlapping bands, some sharp, some diffuse which are also likely Rydberg series members, but are too complicated to positively identify.

There is an extensive continuum from approximately 1300 to 2100Å that partially overlaps the B state and some of the C state. This is very likely caused by a direct dissociation process in either or both of the following reactions.
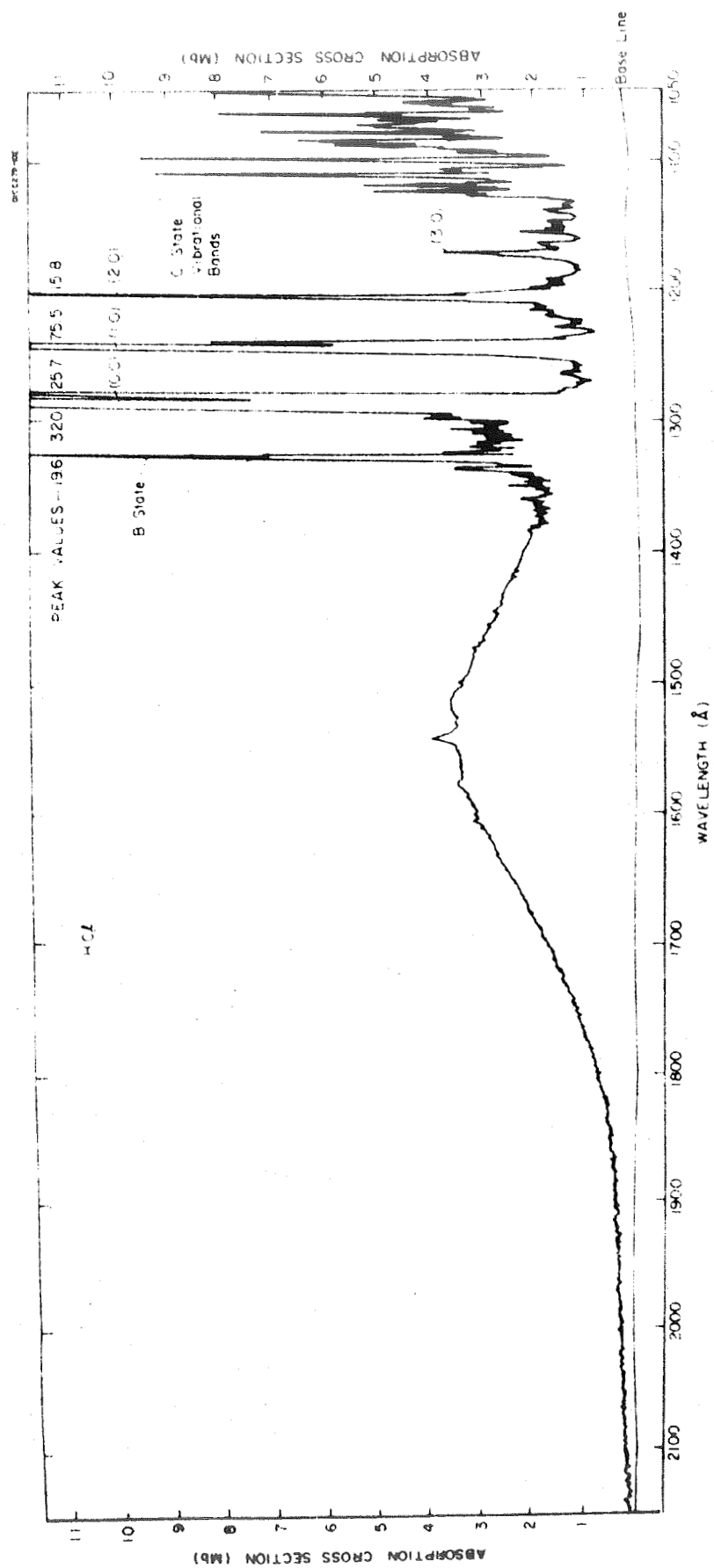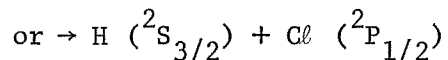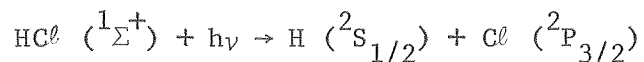
20

Figure 10. Absorption cross section of HCℓ as a function of wavelength from 1050 to 2150Å.

21

$$HC\ell \ (^1\Sigma^+) + h\nu \rightarrow H \ (^2S_{1/2}) + C\ell \ (^2P_{3/2})$$

$$or \rightarrow H \ (^2S_{3/2}) + C\ell \ (^2P_{1/2})$$

Iodine

The vacuum uv spectrum of I_2 has long been commonly identified and associated with the absorption system in the 1790-2200Å region. In Figure 11 this feature appears to be an absorption continuum composed of two or three overlapping continua. At a slower scan speed (see Figure 12), it can be seen that there appears to be an extensive series of vibrational bands superimposed on top of the apparent continuum. The region from 1780 to 1340Å contains series of very strong and sharp band systems. These bands are resonance systems that are members of the Rydberg series leading to the various ionization states. The region below the ionization limit at 1340Å is composed of continuous absorption with structure superimposed on top of it.

In Figure 12, unambiguous interpretation of this feature is found to be extremely complex. It is very difficult to determine whether it is caused by several overlapping continua with a series of weak and diffuse absorption bands superimposed on top of it or by the overlapping to two weak band systems whose structure is either diffuse or unresolvable with the present resolution. The vibrational spacing of these bands is consistant with that reported for the Cordes bands (Ref. 19), in this spectral region, the upper state of which is still yet to be uniquely assigned. This is an extremely complicated spectrum that will require very high resolution work before it is properly analyzed and interpreted.

The resonance bands from 1780Å down to the ionization limit are very well defined and strong. They are all somewhat similar as they exhibit the same type of vibrational structure. As well as the $v'' = 0$ to $v' = 0, 1, 2, \ldots$ n absorption progression, iodine has the $v'' = 0, 1, 2, 3$ to $v' = 0$ progression. This is because the upper vibrational levels of the ground state for iodine are partially populated at room temperature. Using the first resonance band at $\sim$ 1740Å, we attempted a previously unobtained vibrational analysis of the upper state. Before attempting this however, we used the bands of the $v' = 0$, $v'' = n$ progression to calculate the vibrational constants of the ground state. It was felt that we could obtain a feeling for the reliability of our calculations for the upper state by comparing our results for the ground state with the reliable values readily available in the literature.
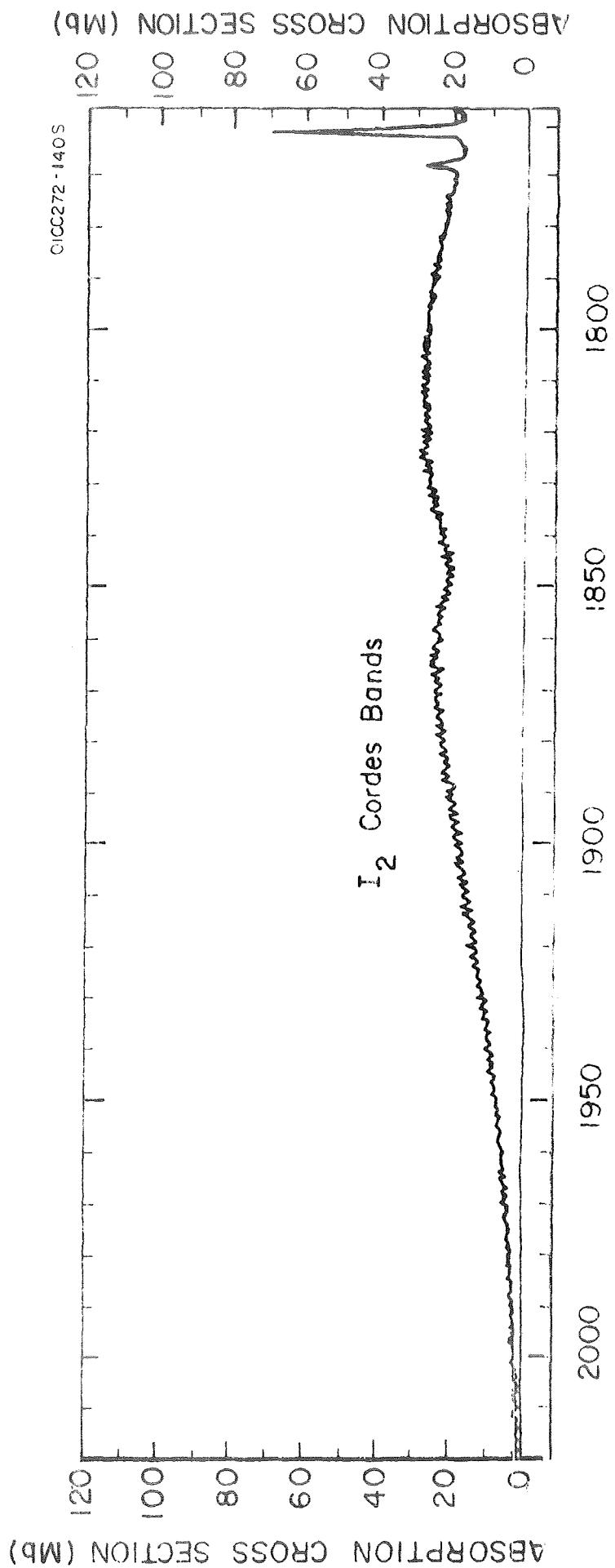
22

Figure 11. Absorption cross section if I_2 as a function of wavelength between 2200 and 1050Å.

23

Figure 12. Absorption cross section of I_2 as a function of wavelength between 2020 and 1760Å.

24

The currently accepted value in the literature of the ground state vibrational frequency ω_e is 214 cm^{-1} (Ref. 12). Our vibrational assignment and calibration yields an ω_e value of 216 cm^{-1} which is definitely within experimental error at the present resolution. Performing the same calculations for the upper state, we calculated an assignment of ω_e = 218 cm^{-1} and $\omega_e x_e$ = 11 cm^{-1}. These values (especially the $\omega_e x_e$) are subject to considerable error as they are derived from the band peaks but they are capable of predicting the peak wavelengths to within better than 0.5Å ($\equiv$ 16 cm^{-1} at 1740Å).

We did not attempt a vibrational analysis of any of the higher lying resonance states as they begin to merge and overlap making a positive identification rather difficult. We were, however, able to identify several members of the Rydberg series leading to the first ionization state (Ref. 20). The ionization limit was calculated to be 75,814 $\pm$ 20 cm^{-1} which corresponds to a wavelength of 1319.02 $\pm$ 0.17Å or 9.4 $\pm$ 0.001 eV. This is in good agreement with the photoionization onset work of Watanabe at 9.82 eV (Ref. 21) and in fair agreement with the photoelectron spectroscopy work of Frost at 9.33 eV (Ref. 22). It is interesting to note on the experimental trace that the Rydberg limit corresponds to an apparent continuum onset. There are also features on the trace that roughly coincide with the higher ionization potentials as measured by Frost (Ref. 22).

Iodine Cyanogen

There has been increased interest in the vacuum uv spectra of ICN, especially, since it has been shown to be a good photochemical source of the CN free radical. Photochemical sources of fragmented radicals have a significant advantage over other discharge or shock tube sources as the energy distribution of the resulting fragments is much easier to control.

CN is an extremely important radical of aeronomical and astronomical interest and for this reason it was decided to measure the vacuum uv absorption cross sections of ICN (see Figure 13).

The spectrum is characterized by two long wavelength photodissociation continua followed by a series of strong resonance Rydberg terms leading to the ionization limits. The first of these continua is found in the region from 2100 to 3000Å and the following reaction has been shown to be in the process responsible for the feature (Ref. 24).

$$ICN + h\nu \ (2100 - 3000\text{Å}) \rightarrow I + CN \ (X^2\Sigma, \ v'' = 0)$$
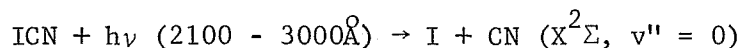
This feature has been designated as the A system and is shown in Figure 14.
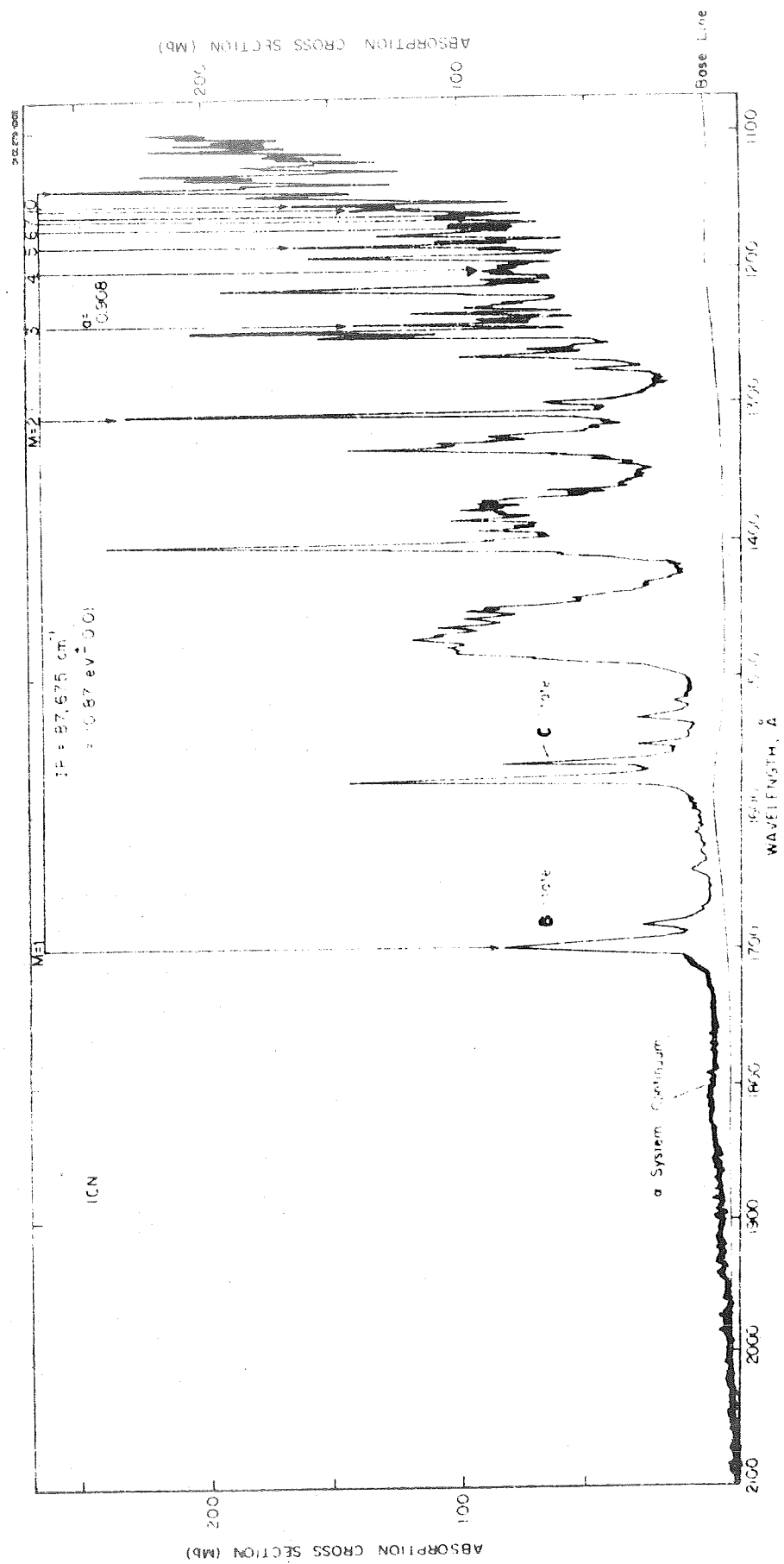
Figure 13. Absorption cross section of ICN as a function of wavelength from 1100 to 2100Å.
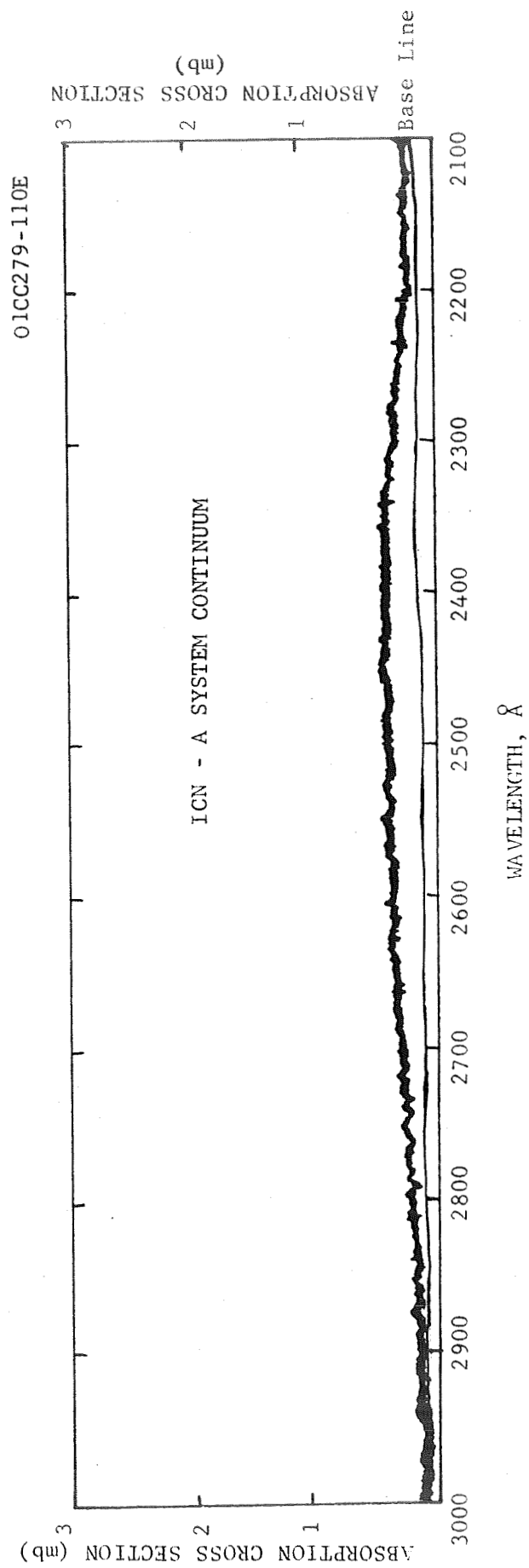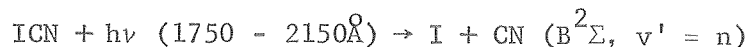
Figure 14. Absorption cross section of ICN as a function of wavelength between 3000 and 2100Å.

The next continuum (the α system) extends from 1750 to 2150Å and has been ascribed to the following reaction mechanism (Ref. 24).

$$ICN + h\nu \ (1750 - 2150\text{Å}) \rightarrow I + CN \ (B^2\Sigma, \ v' = n)$$

The strong bands from 1700Å to the first ionization limit around 1140Å are all very strong Rydberg terms. We were able to analyze the bands to obtain the terms of the first Rydberg series. The wavelengths, quantum numbers and quantum defects of these terms are listed in Table 1. The ionization limit for this series was found to be 1140.6 $\pm$ 0.1Å or 87,675 $\pm$ 8 cm^{-1} or 10.87 eV $\pm$ 0.001 eV. This compares surprisingly well with the value quoted by King and Richardson (Ref. 25) who obtained a value of 87,719 cm^{-1} by using only the first two terms of the series. Usually the quantum defect of the inner-most excited orbitals varies appreciably from the value of the higher terms as we found for the case in I_2, but this effect is not very substantial for ICN. There is only a variation of about 10 percent and this is probably responsible for the good value of the ionization threshold that King reports. Our above quoted value also agrees extremely well with the 10.87 $\pm$ 0.02 eV value found from photoionization studies of Dibeler and Liston (Ref. 26).

The spectrum appears to be too complicated to attempt to identify a second series with the present resolution. There is an apparent continuum onset at about 1180Å which is likely due to a lack of resolution of the strong Rydberg terms as they approach the series limit of the ionization continuum at 1140Å.

TABLE 1

RYDBERG SERIES OF ICN

Wavelength $\lambda(\overset{o}{A})$	Quantum Number $\underline{n}$	Quantum Defect $\underline{a}$
1698.2	1	1.1
1331.3	2	0.91
1241.0	3	0.91
1196.9	4	0.91
1182.9	5	0.91
1171.3	6	0.91
1163.9	7	0.91
1158.9	8	0.91
1155.3	9	0.91
1152.7	10	0.91
1140.6	∞	--

REFERENCES

1. Hudson, R. D. and Carter, V. L., J. Opt. Soc. Am. 58, 227 (1968).

2. Hinteregger, H. E., in Vistas in Astronautics, M. Alperin and M. Stern, Editors (Pergamon Press, New York, 1958), p. 146.

3. Krupenie, P. H., The Band Spectrum of Carbon Monoxide, NSRDS-NBS5 (Superintendent of Documents, U. S. Government Printing Office, Washington, D. C., 1966).

4. Simmons, J. D., Bass, A. M. and Tilford, S. G., Astrophys. J. 155, 345 (1969).

5. Watanabe, K., Zelikoff, M. and Inn, E. C. Y., AFCRL Tech. Rept. No. 53-23, Geophys. Res. Paper No. 21 (1953).

6. Thompson, B. A., Harteck, P. and Reeves, R. R., J. Geophys. Res. 68, 6431 (1963).

7. Tousey, R., Astrophys. J. 149, 239 (1967).

8. Becker, K. H. and Welge, K. H., Z. Naturforschg. 19a, 1006 (1964).

9. Neuimin, H. and Terenin, A., Acta Physicochim, URSS 5, 1 (1936).

10. Watanabe, K. and Sood, S. P., Sc. of Light 14, 36 (1965).

11. Marmo, F. F., J. Opt. Soc. Am. 43, 1186 (1953).

12. Dressler, K. and Miescher, E., Astrophys. J. 141, 1266 (1965).

13. Watanabe, K., Adv. in Geophys. 5, 193 (1958).

14. Driscoll, J. and Warneck, P., J. Phy. Chem. 72, 3736 (1968).

15. Golomb, D., Watanabe, K. and Marmo, F. F., J. Chem. Phys. 36, #4, 958 (1962).

16. Tanaka, I., Carrington, T. and Broida, H. P., J. Chem. Phys. 35, 750 (1961).

17. Price, W. C. and Simpson, D. M., Proc. Roy. Soc. (London) A169, 501 (1938).

18. Price, W. C., Proc. Roy. Soc. (London) A167, 216 (1938).

19. Verma, R., J. Chem. Phys. 32, 738 (1960).

20. Venkateswarlu, P., Bull. Am. Phys. Soc. 14, 622 (1969).

21. Watanable, K., Nakayama, T. and Mottl, J., J. Quant. Spectrosc. Radiat. Transfer 2, 369 (1962).

30

22. Frost, D. C., McDowell, C. A. and Vroom, D. A., J. Chem. Phys. 46, 4255 (1967).

23. Jakovleva, A., Acta Physicochim, URSS, IX, 5 (1938).

24. Jakovleva, A., ibid, X, 3 (1939).

25. King, G. W. and Richardson, A. W., J. Mol. Spect. 21, 339 (1966).

26. Dibeler, V. H. and Liston, S. K., J. Chem. Phys. 47, 11, 4548 (1967).